Effects of physical properties of components on reactive nanolayer joining

J. Wang, E. Besnoin, O. M. Knio, and T. P. Weihs

Citation: Journal of Applied Physics **97**, 114307 (2005); doi: 10.1063/1.1915540
View online: https://doi.org/10.1063/1.1915540
View Table of Contents: http://aip.scitation.org/toc/jap/97/11
Published by the American Institute of Physics

Articles you may be interested in

Room-temperature soldering with nanostructured foils
Applied Physics Letters **83**, 3987 (2003); 10.1063/1.1623943

Reactive nanostructured foil used as a heat source for joining titanium
Journal of Applied Physics **96**, 2336 (2004); 10.1063/1.1769097

Joining of stainless-steel specimens with nanostructured Al/Ni foils
Journal of Applied Physics **95**, 248 (2004); 10.1063/1.1629390

Effect of intermixing on self-propagating exothermic reactions in Al/Ni nanolaminate foils
Journal of Applied Physics **87**, 1255 (2000); 10.1063/1.372005

Modeling and characterizing the propagation velocity of exothermic reactions in multilayer foils
Journal of Applied Physics **82**, 1178 (1997); 10.1063/1.365886

Effect of reactant and product melting on self-propagating reactions in multilayer foils
Journal of Applied Physics **92**, 5474 (2002); 10.1063/1.1509840

HTML ABSTRACT • LINKS

JOURNAL OF APPLIED PHYSICS **97**, 114307 (2005)

Effects of physical properties of components on reactive nanolayer joining

J. Wang[a)]
Department of Materials Science and Engineering, The Johns Hopkins University, Baltimore, Maryland 21218

E. Besnoin and O. M. Knio
Department of Mechanical Engineering, The Johns Hopkins University, Baltimore, Maryland 21218

T. P. Weihs
Department of Materials Science and Engineering, The Johns Hopkins University, Baltimore, Maryland 21218

(Received 7 October 2004; accepted 28 March 2005; published online 24 May 2005)

We studied the effects of the physical properties of components on a reactive joining process that uses freestanding nanostructured Al/Ni multilayer foils as local heat sources to melt AuSn solder layers and thereby bond the components. Stainless-steel reactive joints were compared with Al reactive joints. The strengths of both the stainless-steel and the Al joints increase as the foil thickness and thus the total heat of reaction increases until the foil thickness reaches a critical value. For foils thicker than the critical value, the shear strengths are constant at approximately 48 and 32 MPa for the stainless-steel joints and Al joints, respectively. The critical foil thickness for stainless-steel joining is 40 μm, compared with 80 μm for the joining of Al. Numerical studies of heat transfer during reactive joining and the experimental results suggest that the duration of melting of the AuSn solder is shorter when Al specimens are joined. Thus, a thicker foil is required to enable a sufficient duration (0.5 ms) of melting of the AuSn solder and full wetting of the metallic samples in order to form a strong joint. In general, when components with higher thermal conductivity, higher heat capacity, and higher density are joined, the duration of melting of the solder or braze layer is shorter and therefore a thicker foil is required to ensure the formation of a strong joint.
© *2005 American Institute of Physics*. [DOI: 10.1063/1.1915540]

I. INTRODUCTION

A reactive joining technology has recently been developed that uses nanostructured Al/Ni multilayer foils as local heat sources for soldering or brazing. Self-propagating formation reactions in these foils provide rapid bursts of energy at room temperature[1–5] that can heat and melt the surrounding solder or braze layers and join materials.[6–10] Based on their very localized and rapid heating, reactive multilayer foils provide a unique opportunity to dramatically improve conventional soldering or brazing technologies: reactive foil soldering can be performed at room temperature and thus eliminates the need for external heat sources such as furnaces. Temperature-sensitive components or materials can be joined without thermal damage, and materials with very different coefficients of thermal expansion, e.g., metal and ceramics, can also be joined.

It has been reported that Au-coated stainless-steel 316L specimens can be joined using freestanding Al/Ni reactive foils and AuSn solder layers, offering a shear strength of 48 MPa.[7] It was also suggested that the reactive foil needs to be at least 40 μm thick so that enough heat is released to enable the melting of the solder layers for over 0.5 ms to wet the components and thereby form a strong joint. Stainless-steel 316L has a relatively low thermal conductivity at 16.2 W/mK, compared with common Al alloys and Cu alloys where thermal conductivities range between 100 and 400 W/mK. One concern in the reactive joining of these more thermally conductive materials is that the heat released from the reactive foils will be conducted into the components at a faster rate and the intervening solder layers might not be heated sufficiently to enable a complete melting, a sufficient duration of melting, and an effective wetting of the components. Other physical properties of components, such as heat capacity and density, might also affect the heat transfer and the reactive joining process.

This paper aims at studying the effect of the thermal conductivity, heat capacity, and density of components when performing reactive multilayer joining. The joining of a stainless-steel 316L alloy, using freestanding Al/Ni foils and AuSn solder layers, is compared with the joining of an Al 6061 alloy, with the same reactive foils and solder layers. The thicknesses of the reactive foils were varied in order to determine the minimum foil thickness that is required to form a strong joint for both the stainless-steel and Al components. The resulting microstructures were examined and heat transfer during the reactive joining was studied numerically to predict the melting durations, cooling rates, and local temperatures within the AuSn solder layers. Based on the experimental and numerical results, the effect of thermal conductivity, heat capacity, and density of components on reactive joining is elucidated.

[a)]Electronic mail: jwang@jhu.edu

 © 2005 American Institute of Physics

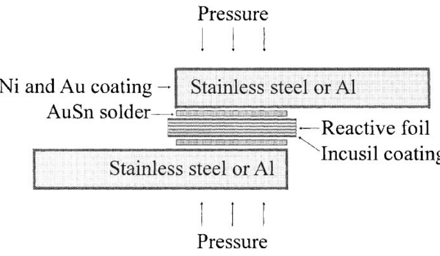

FIG. 1. Schematic showing the reactive joining of stainless-steel and Al shear-lap specimens. The stainless-steel and Al specimens were coated with a Ni and Au metallization. The joints were made using Incusil-coated Al/Ni reactive foils and AuSn solder layers under an applied pressure of 100 MPa.

II. EXPERIMENTAL AND NUMERICAL METHODS

Reactive multilayer Al/Ni foils with an overall 1:1 atomic ratio of Al to Ni were fabricated by magnetron sputtering many alternating Al and Ni layers onto cooled brass substrates that were rotated in front of Al [Al–0.7 wt % (Si,Fe)–0.1 wt % Cu] and Ni (Ni–7 wt % V) targets. To enhance the wetting of the foils by the AuSn solder during joining, a 1-μm-thick wetting layer of Incusil braze (59 wt % Ag–27.25 wt % Cu–12.5 wt % In–1.25 wt % Ti) was deposited on both sides of the Al/Ni multilayers. More details about the sputtering process can be found in a previous paper.[6] Following deposition, the reactive multilayer foils were removed from the brass substrates for use as freestanding foils. The foils used in this study were obtained from two separate sputtering runs. For the first run, the foils contained 640 Al/Ni bilayers with bilayer thicknesses ranging from 25 to 90 nm and total foil thicknesses ranging from 16 to 58 μm. For the second run, the foils contained 2000 Al/Ni bilayers with the same range of bilayer thicknesses (25 to 90 nm) but the total foil thicknesses ranged from 50 to 180 μm.

To characterize the reaction products, freestanding Al/Ni foils were ignited in air and then were ground into powders for x-ray-diffraction (XRD) examination. As-deposited freestanding Al/Ni foils were also examined by XRD for comparison. The heats of reaction of these foils were measured using a Perkin Elmer differential scanning calorimeter (DSC), by heating the freestanding foils (without Incusil braze coating) from 50 to 725 °C at a rate of 40 °C/min and integrating the net heat flow with respect to time. The reaction velocities were measured using a series of optical fibers that are illuminated sequentially as the reactions propagate in front of the fibers, as described earlier.[7,11]

For joining, two 25-μm-thick AuSn solder (80 wt % Au–20 wt % Sn) layers and one reactive foil with thickness ranging from 20 to 180 μm were stacked between two stainless-steel (316L) or Al (6061-T6) samples, as shown schematically in Fig. 1. The stainless-steel and Al specimens, with dimensions of $0.5 \times 6 \times 25$ mm^3 were electroplated with a bilayer Ni/Au metallization to enhance the wetting by the molten AuSn solder. The reactive joining of all the samples was performed at room temperature and in air by igniting the reactive foils under an applied pressure of approximately 100 MPa. The resulting joint areas were approximately 5×6 mm^2 for the stainless-steel joints and

TABLE I. Physical properties of materials used in this study. Relevant parameters also include the solidus and liquidus temperatures of Incusil, respectively, T_s=878 K and T_l=988 K, the heat of fusion of Incusil, H_f=10792 J/mol, the solidus and liquids temperatures of the Au–Sn solder, respectively, T_s=553 K and T_l=553 K, and the heat of fusion of Au–Sn, H_f=6188 J/mol.

Material	Thermal conductivity (W/mK)	Heat capacity (J/kg K)	Density (kg/m^3)
Stainless steel 316L	16.2	500	7990
Al-6061-T6	167	896	2700
AuSn	57	170	14 510
Incusil-ABA	70	276	9700
Al/Ni Foil	152[a]	830[a]	5500

[a]These values were estimated according to the physical properties of Al and Ni target materials.

3×6 mm^2 for the Al joints. The smaller joint area was used for the Al specimens to avoid deformation or fracture of the Al specimens themselves before the failure of the solder joint, due to the low tensile strength of the Al 6061 alloy.

After reactive joining, these stainless-steel and Al joints were shear-lap tested in tension at room temperature using an Instron testing machine and a crosshead speed of 0.1 mm/min. The shear strengths of these joints were obtained by dividing the maximum failure load by the joint area. In order to understand the failure mechanism of these joints, fracture surfaces of the tested stainless-steel and Al joints were observed using a stereomicroscope and chemical analysis of the fracture surfaces of the joints was performed using energy dispersive x-ray (EDX) analysis. Cross sections of untested stainless-steel and Al joints were polished and then characterized using a JEOL scanning electron microscope (SEM).

A numerical study was performed to predict the fraction of the AuSn solder layer that melts during joining as the foil thickness is increased from approximately 20 to 250 μm for both the stainless-steel joining and the Al joining. The duration of the melting of the AuSn solder at the solder/component interface was also predicted, along with the maximum temperature at the solder/component interface and the cooling rate within the solder layer.

To perform the numerical predictions, thicknesses and properties of the foil, solder, and components, such as thermal conductivity, heat capacity, and heat and velocity of reaction, were incorporated into the model, along with an approximate thermal resistance for the unbonded interfaces. Some of the physical properties of the materials used in this study are shown in Table I. The two-dimensional (2D) model is based on a simplified description of the one-dimensional motion of self-propagating reactions that relates the nanoscale transport and kinetic phenomena within the foil, which govern the self-propagation, with the thermal transport and phase evolution, which occur in the AuSn solder layers and the stainless-steel and Al components. Our computation focuses on simulating heat flow into the solder layers, phase changes within these layers, and temperature evolution within the bonded components. The temperature evolution can be obtained by integration of the energy conservation

equation, which is independently solved within the reactive foil, solder layers, and stainless-steel and Al components:

$$\rho \frac{\partial h}{\partial t} = \nabla q + \dot{Q}, \quad (1)$$

where ρ and h are the density and enthalpy of the corresponding layer, t is time, q is the heat flux vector, and $\dot{Q}$ is the heat release rate. The enthalpy h is related to the temperature T through a relationship that involves the material's heat capacity c_p and latent heat h_f. The term $\dot{Q}$ represents the rate of heat release by the self-propagating front as it traverses the reactive foil. Note that $\dot{Q}$ is localized within the front that traverses the foil. More details about the model can be found elsewhere.[7]

III. RESULTS

A. Characterization of reactive foils

XRD scans for as-deposited Al/Ni foils show that all major peaks correspond to Al and Ni. For reacted Al/Ni foils, all major peaks correspond to the ordered $B2$ AlNi compound, which is the equilibrium compound for this composition. Thus, when the foils are reacted during joining, the ordered $B2$ AlNi compound is expected to be the dominant product.

The heat of reaction ΔH increases from 1016 to 1200 J/g as the bilayer thickness increases from 25 to 80 nm, suggesting that a noticeable degree of atomic intermixing occurs at the Al/Ni interfaces during deposition and leads to heat losses and consequently a reduction in the measured heats of reaction for foils with thinner bilayer thickness.[12] We assume that there is a fixed thickness of atomic intermixing between layers and heat losses are proportional to $2w/\lambda$, where w is the intermixing thickness between each layer and λ is the bilayer thickness. By linearly fitting the measured heats of reaction versus the $1/\lambda$ data, we estimated that the maximum heat of reaction ΔH_0 is 1268 ± 21 J/g, and the intermixing thickness w is 2.3 ± 0.3 nm. With these calculated values of ΔH_0 and w, heats of reaction can be calculated for all the bilayer thicknesses. These calculated heats of reaction were used as inputs for the numerical predictions of heat transfer during reactive joining. Reaction velocities were found to increase from 3.5 to 7 m/s as the bilayer thicknesses decreased from 90 to 25 nm, as expected. These velocity data were also used as inputs for the numerical modeling.

B. Numerical results

1. Amount and duration of melting of solder layers in stainless-steel joints and Al joints

Figure 2 shows that the amount of the AuSn solder that melts increases with increasing foil thickness for both the stainless-steel joining and the Al joining. For reactive joining of stainless steel, the amount of the AuSn solder that melts increases from 0 to 25 μm as the foil thickness rises from 0 to 22 μm. For foils thicker than 22 μm, the whole 25 -μm-thick AuSn solder layer melts, which is needed for bonding. The minimum foil thickness needed to melt the full

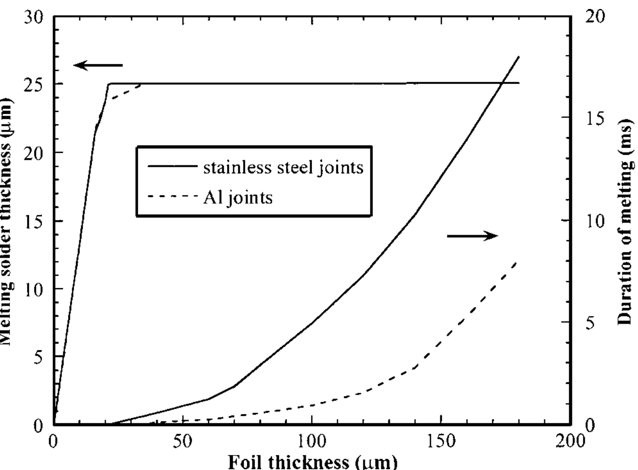

FIG. 2. Numerical predictions of the thickness of AuSn solder that melts and the duration of melting at the solder/component interface as a function of foil thickness.

25-μm-thick Au–Sn solder layer is 35 μm for the Al joints, more than 50% larger than for the stainless-steel samples.

Figure 2 also shows that the duration of melting of the complete AuSn solder layer increases with increasing foil thickness. For the stainless-steel joints, as the foil thickness increases from 22 to 180 μm, the duration of the melting of the AuSn solder layer rises from 0 to 18 ms. For the Al joints, the duration of melting is much shorter and increases from 0 to only 8 ms as the foil thickness increases from 35 to 180 μm. This difference in the duration of melting is due mainly to the higher thermal conductivity of Al (167 W/mK) compared with stainless steel (16.2 W/mK). Al specimens simply enable faster dissipation of heat from the AuSn solder during joining.

2. Temperatures and cooling rates in stainless-steel joints and Al joints

Figure 3 shows that the maximum temperatures at the solder/component interfaces increase with increasing foil thickness for both stainless-steel joining and Al joining, as

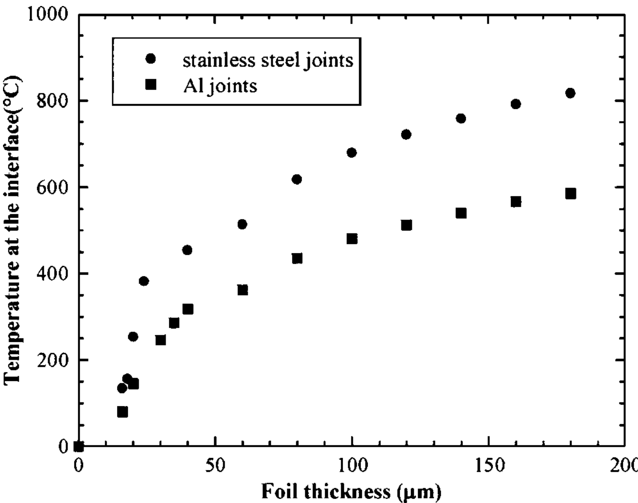

FIG. 3. Numerical predictions of the temperatures at the solder/component interface as a function of foil thickness.

FIG. 4. Temperature vs time at the center of AuSn solder layers in stainless-steel and Al joints made with 80-μm-thick Al/Ni foils and 25-μm-thick AuSn solder layers obtained from numerical prediction.

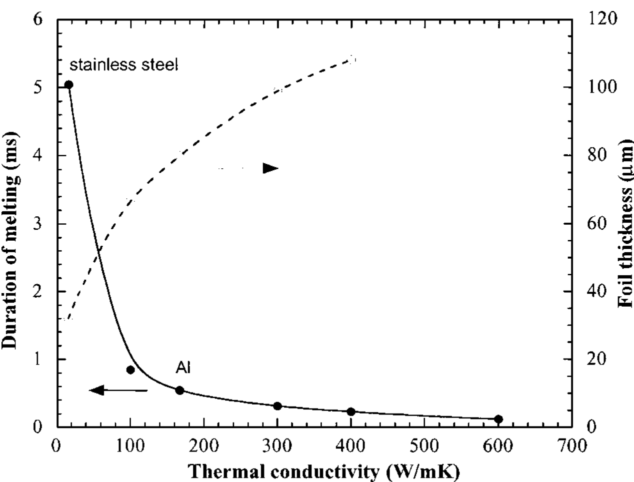

FIG. 5. Numerical predictions of the duration of melting for joining with 80-μm-thick foils and critical foil thickness required to enable a melting duration of the AuSn solder of 0.5 ms as functions of thermal conductivity of components. All other physical properties of components are assumed to be those for Al 6061. The thermal conductivity data for stainless steel and Al are marked in the plot.

expected. For the joining of stainless steel, as the foil thickness increases from 17 to 180 μm, the maximum temperatures at the solder/stainless-steel interfaces increase from 25 to 820 °C. The maximum temperatures at the solder/Al interfaces are much lower. As the foil thickness increases from 16 to 180 μm, the maximum temperatures at the interfaces rise from 25 to only 590 °C.

Figure 4 shows temperatures versus time at the center of the AuSn solder layer in both a stainless-steel joint and an Al joint made with two 25-μm-thick AuSn solder layers and one 80-μm-thick Al/Ni foil. Following the reaction of the foil, the temperature at the center of the solder layer in the stainless-steel joint decreases from 700 to 400 °C within 1 ms, with a maximum cooling rate of 0.7×10^6 °C/s. It takes 3 ms for the center of the solder layer to cool down to its melting temperature, 280 °C, with a cooling rate of 2×10^4 °C/s at the point of solidification. The Al joint cools faster than the stainless-steel joint and the temperature at the center of the solder layer decreases from 600 to 260 °C within 1 ms, with a higher maximum cooling rate of 1.1×10^6 °C/s. It takes 0.7 ms for the center of the solder layer to cool down to its melting temperature, with a cooling rate of 1.1×10^5 °C/s at solidification.

3. Effect of thermal conductivity, heat capacity, and density on duration of melting

To more directly assess and isolate the effects of the physical properties of components on reactive multilayer joining, the duration of melting of the AuSn solder layers was predicted for joining materials with a wide range of thermal conductivities, heat capacities, and densities.

Firstly, only the thermal conductivity is varied and other physical properties are assumed to be those for Al (6061-T6). As seen in Fig. 5 the melting of the solder layer is very sensitive to the thermal conductivity of the components. The duration of melting decreases from 5 to 0.1 ms as the thermal conductivity of the components increases from 16 to 600 W/mK for an 80-μm foil. Conversely, to ensure a duration of melting of at least 0.5 ms as the thermal conductivity of components increases from 16 to 400 W/mK, the minimum foil thickness rises from 32 to 108 μm.

The energy conservation equation [Eq. (1)] that was used to solve the temperature evolution within the foil, solder layers, and stainless-steel and Al components can also be expressed as

$$\rho C_p \frac{\partial T}{\partial t} = \nabla q + \dot{Q}, \tag{2}$$

where ρ and C_p are the density and heat capacity of the corresponding layer, and T is the temperature. It can be seen from Eq. (2) that the temperature evolution in each layer and the duration of melting in solder layers are also dependent on the density and heat capacity of components.

Figure 6 shows that when thermal conductivity and density are assumed to be those for Al (6061-T6), which are 167 W/mK and 2700 kg/m^3, respectively, the duration of melting of the solder layers decreases dramatically from 1.74 to only 0.29 ms (solid circles in Fig. 6) as the heat capacity of components increases from 300 to 2000 J/kg K. Thus thicker foils are required to maintain a minimum melting duration of 0.5 ms as heat capacity increases. Similarly, varying only the densities of components from 600 to 5000 kg/m^3, the duration of melting of the solder layer decreases from 2.59 to 0.35 ms (solid squares in Fig. 6). Thus, again thicker foils are required as density increases.

Although there is no specific relationship between heat capacity and density, materials with higher densities tend to have lower heat capacities. Thus, we examined the effect of the product of heat capacity and density on the duration of melting of the solder layers, as the thermal conductivity of components varies from 10 to 400 W/mK (Fig. 6). When the product of heat capacity and density increases, the duration of melting of the solder layers decreases gradually. It is also clear in Fig. 6 that for a given product of heat capacity and density, a higher thermal conductivity will result in a

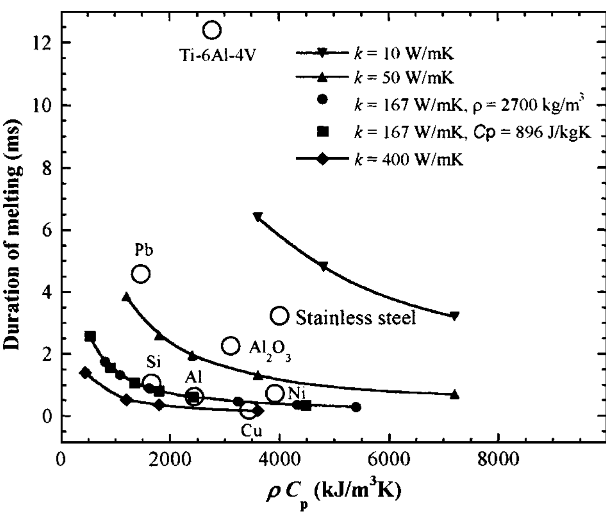

FIG. 6. Numerical predictions of the duration of melting as a function of the product of the heat capacity and the density of components, as thermal conductivity varies from 10 to 400 W/mK. The foil thickness is 80 μm. Melting durations for joining some commonly used materials are calculated and labeled in this plot.

shorter melting duration, as expected. Melting durations for joining some commonly used materials are calculated and labeled in this plot. Note that the product of density and heat capacity of stainless steel is higher than that of Al alloy, but the thermal conductivity of stainless steel is much lower than that of Al, and the melting duration in stainless-steel joining is more than five times longer than that in Al joining. When comparing stainless-steel joining and Al joining, the thermal conductivities of components are the dominant factors in determining the duration of the melting of the solder layers.

C. Microstructural and mechanical characterizations

During reactive joining, cracks were formed within the reacted foil and most of the molten solder flowed into cracks and out of the joining area, due to the large applied pressure. The AuSn solder layers decreased in thickness from 25 μm to several microns.[6,7] The microstructures of the AuSn solder in a stainless-steel joint and an Al joint, both made with 80-μm-thick Al/Ni foils and 25-μm-thick AuSn solder layers, are shown in Figs. 7(a) and 7(b). In both stainless-steel and Al joints, a very fine lamellar eutectic structure is observed, including a light Au-rich phase and a dark Sn-rich phase. The formation of the fine lamellar structure is due to the very rapid cooling of the reactive joint. The lamellar spacings of the AuSn solder in the stainless-steel joint and the Al joint are approximately 30 and 20 nm, respectively.

Figure 8 shows that shear strengths of stainless-steel and Al joints increase as the foil thickness increases, until the thickness of the foil reaches a critical value. Further increases in the foil thickness do not affect the shear strength of the joints. For the stainless-steel joints, the critical foil thickness is 40 μm. For thicker foils the average value is 48 ± 3 MPa. For the Al joints the critical foil thickness is 80 μm and the average value above 80 μm is only 32 ± 5 MPa.

Previous observations of fracture surfaces of stainless-steel joints revealed that when the reactive foil is very thin,

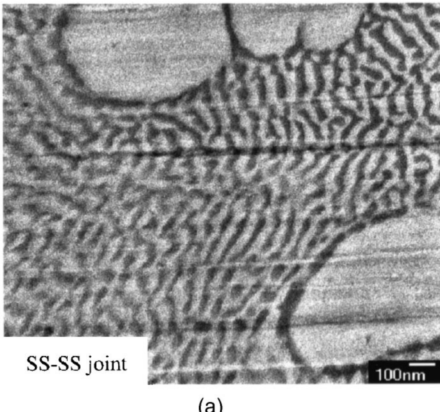

(a)

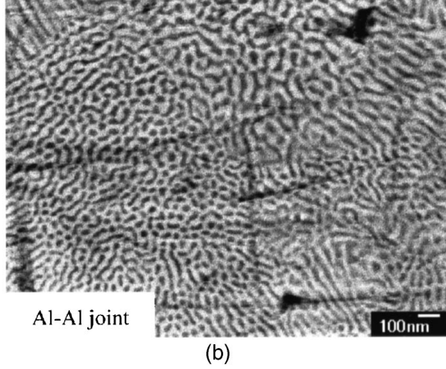

(b)

FIG. 7. Fine lamellar eutectic structure of AuSn solder (a) in a stainless-steel–stainless-steel joint, with a lamellar spacing of 30 nm, and (b) in an Al–Al joint, with a lamellar spacing of 20 nm. Both the stainless-steel and the Al joints were made with 80-μm-thick foils.

e.g., 23 μm, the duration of melting is very short and there is little wetting of the stainless-steel specimens. As the thickness of the reactive foil increases, the duration of melting of the AuSn solder rises and there is more wetting of the specimens. When the reactive foil is sufficiently thick, the duration of melting of the AuSn layers is long enough to enable a complete wetting of the stainless-steel specimens. For joints made with foils thicker than 40 μm, EDX analysis shows

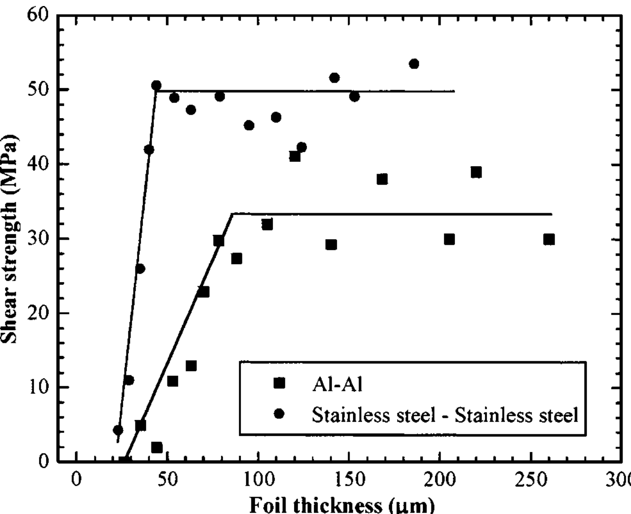

FIG. 8. Shear strength of stainless-steel joints and Al joints as a function of foil thickness.

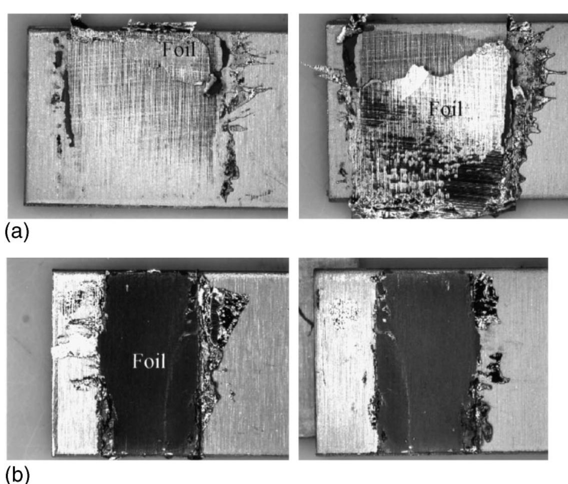

FIG. 9. Fracture surfaces of the Al joints obtained by optical stereomicroscopy: (a) joint formed with a 35-μm foil, showing very limited wetting of the Al components, and (b) joint formed with a 120-μm foil with full wetting of the Al components.

that Au and Sn are the dominant elements on both sides of the stainless-steel fracture surfaces, indicating that failure occurred in the AuSn solder.[7] For comparison, here we studied the fracture surfaces of Al joints. Optical photographs of fracture surfaces are shown in Fig. 9. When a 35-μm-thick foil was used, there is a very limited wetting of the Au-coated Al specimen [Fig. 9(a)] and failure occurred at the interface between the AuSn solder and the Au-coated Al specimen. Using a thicker foil, e.g., 120 μm, both fracture surfaces are uniformly dark [Fig. 9(b)], and indicate good wetting of the Al specimens by the AuSn solder. However, in this case failure did not occur within the AuSn solder. The EDX analysis shows that Al is the dominant element on one side of the joint where no foil remains, and Al and Ni are the dominant elements on the other side of the joint where the reacted foil is attached. Au and Sn were observed only beyond the joining area and are assumed to be extruded solder. The lack of solder on fracture surfaces suggests that the fracture occurred at the interface between the Al specimen and the Ni undercoating layer. SEM observations show ductile fracture of Al at the nonfoil side of the joint and both ductile fracture of Al and detached Ni coating at the foil side. This confirms that failure occurred at the interface between the Al component and the Ni electroplating, which is weaker than the interface between the AuSn solder and the Au coating, in the case of complete wetting.

IV. DISCUSSION

As shown in Fig. 8, the maximum shear strength of the Al joints is lower than that of the stainless-steel joints. This is due to the different fracture modes in these joints. Failure of the stainless-steel joints occurred within the AuSn solder layer, while the Al joints failed at the interface between the electroplated Ni layer and the Al component, suggesting a weak interface between the Au metallization and the Al component. One possibility for the weaker interface in the Al joints is that the Ni underlayer is not wetting the Al surface as well as the stainless-steel surface during plating, probably due to the quicker oxidation of the Al. Thus, during the tensile shear test, the Ni underlayer for the Au metallization debonds from the Al specimen surface. The weaker interface between the Ni underlayer and the Al component might also be attributed to the formation of an Al–Ni intermetallic layer at the Al specimen/Ni underlayer interface during the reactive bonding. The formation of a thin intermetallic layer could embrittle the interface and result in a lower shear strength.

Excluding the case where metallizations are poorly bonded to the base components, shear strengths of reactive joints are controlled by melting and wetting of the solder onto the components. As shown in Figs. 2 and 8, a 20-μm-thick foil and a 35-μm-thick foil are needed to melt the whole 25-μm-thick AuSn solder for the joining of the stainless-steel and Al samples, respectively. Yet, joints made with foils of these thicknesses are very weak. Thus, complete melting of the solder layers is not a sufficient condition for obtaining the maximum shear strength of reactive joints. Shear strength data show that the foils needed to be at least 40 and 80 μm thick to form strong stainless-steel and Al joints, respectively. Numerical results predict that the duration of melting of the AuSn solder layers is approximately 0.5 ms when stainless-steel and Al samples are joined using such foils. From both the shear strength data and numerical predictions, it can be seen that the freestanding solder layers must melt across their complete thickness and remain molten for at least 0.5 ms to ensure good flow of solder, complete wetting of the components, and the formation of a strong joint.

The duration of melting during Al joining is shorter than that during stainless-steel joining when similar foils are used, due to the larger thermal conductivity of Al. Heat is conducted faster into the Al specimens than into the stainless-steel specimens, and AuSn solder cools more rapidly during the reactive joining of Al. Thus thicker foils (at least 80 μm) are needed to melt the AuSn solder for at least 0.5 ms and thereby form a strong joint. Even thicker foils will be needed to join more conductive materials. For example, a 108-μm-thick foil would be needed to join Cu components (400 W/mK). Increases in foil thickness are also required as the heat capacity or the density of the components rises (Fig. 6).

The differences in the thermal conductivities of stainless steel and Al also lead to different maximum temperatures at the solder/component interfaces and differences in cooling rates following reactive joining. The differences in maximum temperatures could impact the wetting and shear strength of reactive joints, but such effects could not be confirmed here. What was confirmed is that the higher cooling rates in the Al joints lead to finer microstructures than in the stainless-steel joints, as seen in Fig. 7. Even finer microstructures are expected when joining more conductive materials like Cu. The finer microstructures in the solder layers should in turn increase joint strength, if failure occurs in the solder layer.[7]

As noted earlier, and as demonstrated here, the melting of the AuSn solder layer is more dependent on thermal transport factors than the thermodynamic requirements for melt-

ing. For example, the heat Q needed to melt a unit area of the AuSn solder layers can be determined by a thermodynamic calculation,

$$Q = \rho t(T_m - T_{\mathrm{RT}})C_p + \rho t \Delta H_f, \tag{3}$$

where ρ and t are the density and total thickness of the AuSn solder layers, T_m is the melting temperature of the AuSn solder, T_{RT} is room temperature, C_p is the heat capacity of the AuSn solder, and ΔH_f is the heat of fusion of the AuSn solder (J/g). The heat needed to melt a unit area of AuSn solder layers with a total thickness of 50 μm was calculated to be 55 $\mathrm{kJ/m^2}$. The heats released from the reactive foils for the joining of the stainless-steel and the Al specimens were 300 and 500 $\mathrm{kJ/m^2}$, respectively, for 40 and 80 μm foils. (Note that the 40 and 80 μm foils contain different bilayer thicknesses so that the total heat from the 80 μm foils is less than twice the heat from the 40 μm foils.) The much larger energy in the foils demonstrates that the physical properties governing heat transport into the solders and components play a larger role during reactive joining than the thermodynamic requirements for melting.

V. CONCLUSIONS

In conclusion, we studied the reactive joining of stainless-steel specimens and Al specimens using freestanding Al/Ni nanostructured multilayer foils and AuSn solder layers. The use of thicker foils increases the available heat and improves the strength of the joints, until a critical thickness is reached. Above that critical thickness the shear strength is approximately constant. The critical thicknesses for stainless-steel joints and Al joints are 40 and 80 μm, respectively. Numerical predictions of the melting of the AuSn solder layers and the experimental measurements of the shear strength indicates that the AuSn solder layers need to melt through their full 25 μm thickness and be molten for at least 0.5 ms to ensure a full wetting and establish strong joints for both stainless-steel specimens and Al specimens. Numerical results also suggest that under the same condition, the duration of melting of the AuSn solder is shorter when materials with higher thermal conductivity, higher heat capacity, and higher density are joined, resulting in a thicker critical foil thickness.

ACKNOWLEDGMENTS

This work was supported by the National Science Foundation through Award DMI-0115238, and by Agilent Technologies, Inc.

[1] E. Ma, C. V. Thompson, L. A. Clevenger, and K. N. Tu, Appl. Phys. Lett. **57**, 1262 (1990).
[2] L. A. Clevenger, C. V. Thompson, and K. N. Tu, J. Appl. Phys. **67**, 2894 (1990).
[3] A. J. Gavens, D. V. Heerden, A. B. Mann, M. E. Reiss, and T. P. Weihs, J. Appl. Phys. **87**, 1255 (2000).
[4] U. Anselmi-Tamburni and Z. A. Munir, J. Appl. Phys. **66**, 5039 (1989).
[5] T. S. Dyer and Z. A. Munir, Scr. Metall. Mater. **30**, 1281 (1994).
[6] J. Wang *et al.*, Appl. Phys. Lett. **83**, 3987 (2003).
[7] J. Wang, E. Besnoin, A. Duckham, S. J. Spey, M. E. Reiss, O. M. Knio, and T. P. Weihs, J. Appl. Phys. **95**, 248 (2004).
[8] A. Duckham, E. Besnoin, S. J. Spey, J. Wang, M. E. Reiss, O. M. Knio, and T. P. Weihs, J. Appl. Phys. **96**, 2336 (2004).
[9] J. Wang, E. Besnoin, O. M. Knio, and T. P. Weihs, Acta Mater. **52**, 5265 (2004).
[10] S. J. Spey, E. Besnoin, A. Duckham, J. Wang, O. M. Knio, and T. P. Weihs, J. Am. Ceram. Soc. (submitted).
[11] M. E. Reiss, C. M. Esber, D. V. Heerden, A. J. Gavens, M. E. Williams, and T. P. Weihs, Mater. Sci. Eng., A **261**, 217 (1999).
[12] T. P. Weihs, *Handbook of Thin Film Process Technology* (IOP, Bristol, UK, 1998).